Fast-switching chiral nematic liquid-crystal mode with polymer-sustained twisted vertical alignment

Kai-Han Chang,* Vinay Joshi, and Liang-Chy Chien
Liquid Crystal Institute and Chemical Physics Interdisciplinary Program, Kent State University, 1425 Lefton Esplanade, Kent, Ohio 44242, USA

(Received 26 September 2016; revised manuscript received 21 January 2017; published 18 April 2017)

We demonstrate a fast-switching liquid-crystal mode with polymer-sustained twisted vertical alignment. By optimizing the polymerization condition, a polymer microstructure with controlled orientation is produced. The polymer microstructure not only synergistically suppresses the optical bounce during field-induced homeotropic-twist transition but also shortens the response time significantly. Theoretical analyses validate that the ground state free energy density is modified by the aligning field of the polymer microstructure, which affects the driving voltage of the device. The outcomes of this paper will enable the development of fast-switching and achromatic electro-optical and photonic devices.

DOI: 10.1103/PhysRevE.95.042701

Liquid crystals (LCs), the fourth state of materials, have been used for applications related to optical modulation thanks to their anisotropic dielectric and optical properties. The orientation of rodlike LC molecules can be modulated by external electric or magnetic field. The effective refractive index and phase retardation depend on the orientation of LC molecules, the thickness of the LC layer, and the polarization of incident light. Furthermore, LCs can be operated with low power consumption with response time at milliseconds scale, which makes it the most widely used material for the display application.

A chiral nematic liquid-crystal mode with homeotropic alignment and negative dielectric anisotropy was proposed in 1993 [1–3]. A liquid-crystal cell with homeotropic alignment is injected with a negative liquid crystal and a small quantity of chiral dopant and placed between crossed polarizers. At field-off state, the liquid-crystal molecules are vertically aligned, which gives a good dark state thanks to the absolute zero phase retardation from the liquid-crystal layer. In the presence of an electric field, the liquid-crystal director forms a twist structure and enables the light to pass through. This mode provides excellent contrast ratio because of the good dark state of the vertical aligned (VA) mode and has the benefit of wavelength dispersion suppression characteristic of twisted-nematic (TN) structure. This mode can be used in both transmissive and reflective displays [4]. By changing the ratio between cell gap d and cholesteric pitch p (d/p), this mode can be further applied onto development of bistable displays [5,6] and guest-host devices [7,8].

The drawback that prevents this director configuration from real world application is the slow dynamic response resulting from pretilt angle degeneracy at the instance when the external field is applied. The pretilt angle degeneracy induces the disclination defects, which take a long time to annihilate (70–90 ms) [9,10]. The optical bounce that arises from the backflow also contributes to the slow response as well as flickering. This slow dynamic response can be solved by switching it from a warm-up voltage (V10, voltage for switching the device to 10% transmittance) instead of zero. However, the tradeoff of this solution is higher power consumption.

In this paper, we report a liquid-crystal mode with polymer-sustained twisted vertical alignment (PS-TVA), inspired by the polymer-stabilized liquid-crystal devices which have significantly improved the dynamic response [11–14]. The schematic is as shown in Fig. 1, where the green grains and fibers represent polymer structure pinned at the surface of substrates and extended into bulk and yellow-colored ellipsoids are liquid-crystal molecules. The PS-TVA effectively solves two key issues that result in a slow rise time of the TVA mode and enhance the decay time at the same time. We report the effect of applied voltages during polymerization on the electro-optical (EO) responses. The effective aligning field from the polymer structure modifies the free energy at the field-off state, and further affects the EO response.

The formulated mixture of a photopolymerizable chiral nematic liquid crystal consists of a nematic liquid crystal with a negative dielectric anisotropy (99.362%, $\Delta\varepsilon = -3.4$, $\Delta n = 0.098$, $K_{11} = 14.9\,\text{pN}$, $K_{33} = 15.9\,\text{pN}$, Merck), a chiral dopant R5011 (0.038%, HCCH, China), and a reactive monomer RM257 (0.6%, HCCH, China). The purpose of using a low concentration of reactive monomer is to minimize indices mismatching between liquid crystal and polymer. The helical pitch p_0 of this mixture is 19.2 μm measured with the Cano-wedge cell method [15]. The formulated mixture of a traditional TVA mode for comparison consists of the same negative nematic liquid crystal (99.962%, Merck) and a chiral dopant R5011 (0.038%). The mixture is injected into liquid-crystal cells coated with a vertical alignment layer (SE-1211, Nissan Chemical Industries) on both top and bottom substrates. The alignment layers are rubbed and the substrates are assembled in an antiparallel configuration with respect to the rubbing directions. The EO cells have a patterned electrode area of 5 × 5 mm on both substrates. The cell gaps of the liquid-crystal cells are controlled with 5-μm spacers with error tolerance $\pm 0.2\,\mu$m. The light source we use for polymerization is a metal halide lamp (Loctite) with several emission peaks at a wavelength of UV range. The UV light intensity for polymerization is controlled at $35\,\text{mW/cm}^2$ with exposure time of 10–12 min. For polymerization with curing voltage study, the waveform applied onto the cell during polymerization is a square wave with a frequency of 1 kHz.

For EO response measurements, we placed the liquid-crystal cell between a pair of crossed polarizers and aligned

*kchang1@kent.edu

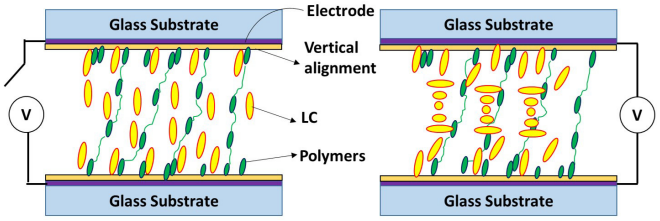

FIG. 1. Operation schematic of PS-TVA mode. Yellow/light gray ellipse, LC; green/dark gray ellipse, polymers.

the rubbing direction parallel to the transmission axis of one of the polarizers crossed at 90 deg. The static voltage response and the dynamic response are measured with a 633-nm HeNe laser. The frequency of the applied electric field is 1 kHz with square waveform. Figure 2(a) is the static voltage response. Without polymer-sustained alignment, the threshold voltage of TVA mode is 2.15 V. With polymer-sustained structure cured at field-off state, the threshold voltage increased 11.6% to 2.4 V. When the curing voltage further increases to larger than threshold voltage, as shown in Fig. 2(a), the threshold voltage decreases (cured at 4 V) and even vanishes if the curing voltage is higher (5 V) because of a large tilt angle deviating from the normal at field-off state. This result suggests that the driving

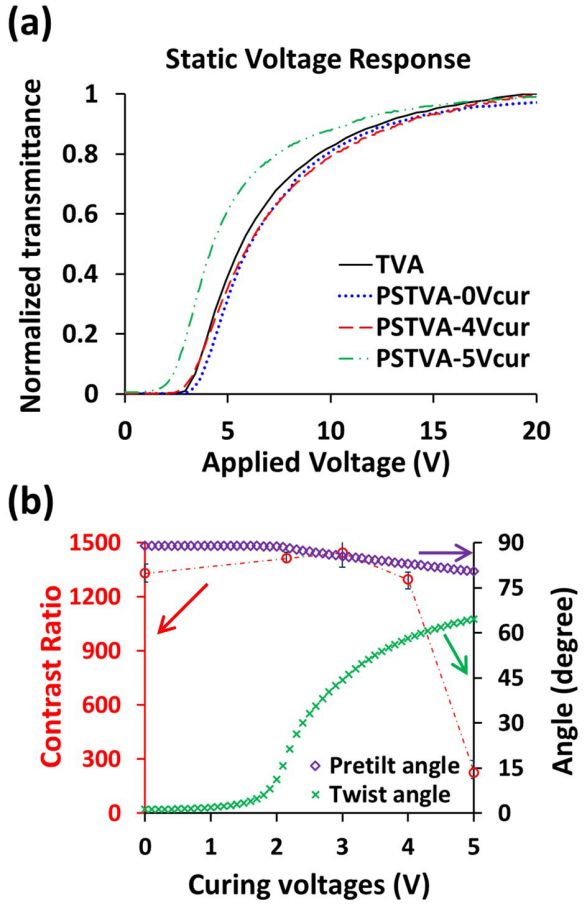

FIG. 2. (a) Static voltage response of TVA and PS-TVA mode with different curing voltages. (b) Contrast ratio of PS-TVA with different curing voltages (red circles) and simulated director profile: pretilt angle (purple diamond) and total twist angle (green cross).

voltage could be lowered if we use a curing voltage that is higher than the threshold voltage of the same material without polymer. However, at a high curing voltage, the polymer-sustained alignment holds the liquid crystals at the high tilt angle away from the normal with a twist structure at field-off state and results in the contrast ratio of PS-TVA cells dropping from ∼1300 : 1 to ∼200 : 1 for curing voltage increasing from 4 to 5 V as shown in Fig. 2(b) (red circles). To evaluate the effect from the pretilt angle and twist structure predefined by the polymer fibers, we simulate the liquid-crystal director with Techwiz 2D (SANAYI system Co., Ltd.) at different curing voltages and extract the pretilt angle and total twist, which experimentally will achieve 90 deg determined by the cell gap to pitch ratio at high voltage. Here we define the pretilt angle as the angle between the molecular axis of the liquid crystal and the surface. With the rubbing direction parallel to the transmission axis of one polarizer, the pretilt angle has less effect on the transmittance of the PS-TVA cell. The total twist angle significantly increases when the applied voltage exceeds threshold voltage. The contrast ratio dramatically drops at the point of total twist angle equal to 60 deg with pretilt angle 82°. The twist structure increases the phase retardation seen by the polarized light and induces rotation of polarization ellipse, and therefore the transmittance increases in comparison with the dark state with curing voltage of 0 V.

The demonstration of the elimination of disclination defects is corroborated by micrographs taken with a polarizing optical microscope (POM) as shown in Fig. 3. Figures 3(a), 3(c), and 3(e) are captured at the field-off state, while Figs. 3(b), 3(d), and 3(f) are captured at the instance when the electric field is applied. Without polymer-sustained alignment, the declination defects appear because of the pretilt angle degeneracy owing to the insufficient anchoring strength from vertical alignment as shown in Fig. 3(b). In contrast, PS-TVA exhibits no defects [Figs. 3(d) and 3(f)] at switching on state and slight light leakage at field-off state [Figs. 3(c) and 3(e)]. The slight light leakage is induced by the scattered polymer structure on the surface. With high applied voltage during polymerization, the scattering light from polymer structure is more severe.

With different curing voltages, the polymer structures freeze the liquid-crystal director at polymerization voltages. The viewing angle can be affected by the defined polymer structure. A simulation of angular-dependent light transmittance of TVA mode at different applied voltages conducted with Techwiz LCD 2D (SANAYI System, Co., Ltd.) is as shown in Fig. 4. The blue numbers are azimuthal observation angles and the black numbers are polar observation angles. The arrangement of the axes of the polarizers and the rubbing direction of the TVA cell in the simulation is the same as the one in the experiment. The electro-optical responses measured in the experiment are at normal incidence, which is at the center of the polar charts in Fig. 4. With the polymerization voltage smaller than the threshold voltage [Figs. 4(a) and 4(b)], TVA mode is at homeotropic alignment state, which exhibits a good dark state along the transmission axes of polarizers (azimuthal direction of 0 and 90 deg in Fig. 4). At the polymerization voltage larger than threshold voltage [Figs. 4(c)–4(f)], when the polymerization voltage is slightly higher than the threshold voltage [Fig. 4(c)], a good dark state remains at normal incidence which is compatible with the experimental results.

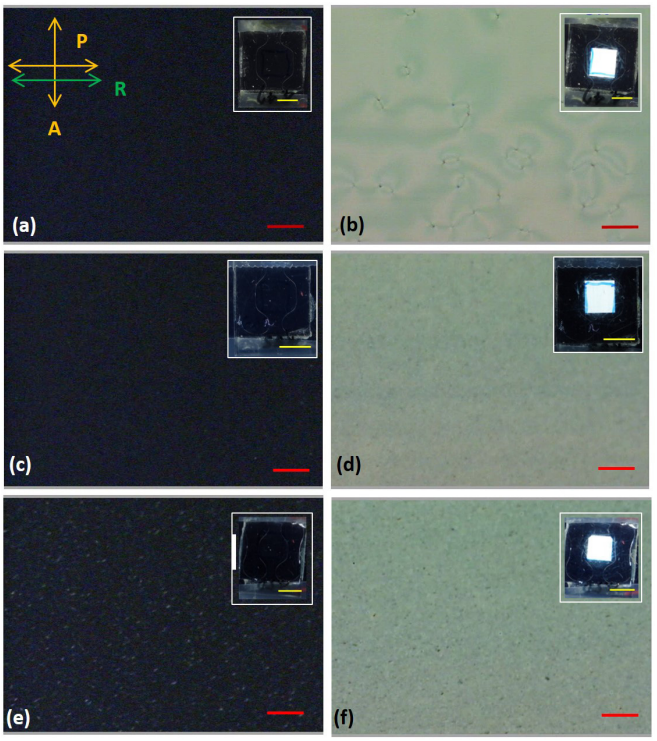

FIG. 3. POM images of (a) TVA mode, 0 V; (b) TVA mode, 14.5 V; (c) PS-TVA mode (V_{cur} = 3 V), 0 V; (d) PS-TVA mode (V_{cur} = 3 V), 13.4 V; (e) PS-TVA mode (V_{cur} = 4 V), 0 V; and (f) PS-TVA mode (V_{cur} = 4 V), 16.9 V. The inserted photos are the corresponded cell images observed under crossed polarizers. The red scale bar in the POM images is 50 μm and yellow scale bar in the inserted photos is 5 mm.

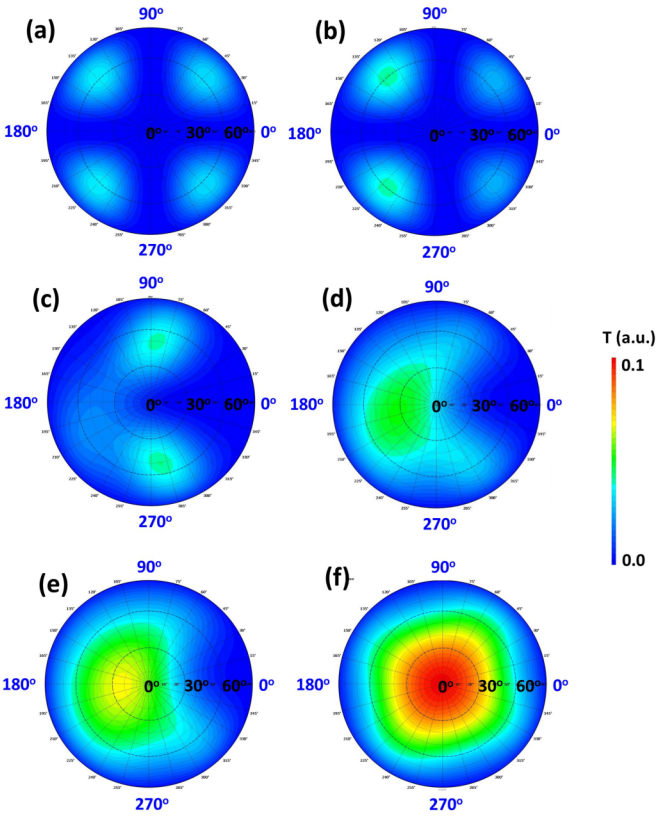

FIG. 4. Angular-dependent light transmittance (T) of TVA mode at different applied voltages: (a) 0 V, (b) 2 V, (c) 3 V, (d) 4 V, (e) 5 V, and (f) 20 V.

At the applied voltage of intermediate state (i.e., the transmittance is not yet at its maximum), a gray scale inversion is observed [Figs. 4(d) and 4(e)] which is similar to the existing twisted nematic mode with planar alignment.

The angular-dependent transmittance of TVA mode [Fig. 4(f)] at field-on state is identical to the twisted nematic cell, and that at field-off state depends on the polymerization voltage. With the polymerization voltage smaller than threshold voltage, the angular-dependent transmittance is identical to an electrically controllable birefringence cell with vertical alignment layers [Figs. 4(a) and 4(b)]. A device with wide angular-independent transmittance area, i.e., large viewing cone with uniform transmittance, has a wide viewing angle. The demonstrated TVA mode in this paper is a single pixel configuration without extra treatment for increasing the viewing angle. To further improve the viewing angle property of TVA mode, one can utilize a multidomain approach [16,17] or applying compensation film [18] which are originally proposed for twisted nematic liquid-crystal cells and vertical alignment modes. The viewing angle property can also be improved by employing a directional backlight and diffuser [19].

The dynamic response is measured with the switching between 0 V and the voltage that gives 90% transmittance. The rise time is defined as the time for transmittance changing from 10 to 90%, and the fall time is defined as the transmittance changing from 90 to 10%. The dynamic responses of TVA and PS-TVA cells with different curing voltages are shown in Figs. 5(a) and 5(b). The dynamic response of PS-TVA cells with curing voltage of 5 V is not compared here because of the low contrast. The optical bounce occurs during the switching from a homeotropic alignment to a twist structure. The optical bounce is suppressed successfully when the curing voltage is higher than the threshold voltage. Without polymer-sustained structure, the rise time is 72.5 ms, while that of PS-TVA mode (curing voltage 4 V) is 7.4 ms. The fall time of TVA mode is 9.7 ms, while that of PS-TVA mode (curing voltage 4 V) is 6.6 ms. With a proper polymerization condition, the issue of long dynamic response time is resolved. The decay time is also shorter with the polymer-sustained alignment thanks to the enhanced restoration torque from the anchoring of the polymer structure. Another interesting phenomenon shown in Fig. 5(a) is that the amplitude of optical bounce is the largest in the PS-TVA sample without curing voltage. The optical bounce of TVA mode is mainly caused by the disappearance process of abnormal twist occurring near the boundaries and the slow equilibrium process of the tilt angle throughout the cell [20]. The backflow effect caused very large variation of the twist angle near the substrates. With the polymer microstructure which strengthens the anchoring parallel to the substrate normal, the competition between the backflow and the anchoring from the polymer may induce larger abnormal twist angle as well as larger tilt angle variation in the transient tilt angle distribution.

The voltage applied during polymerization is a critical element for obtaining fast response time without sacrificing

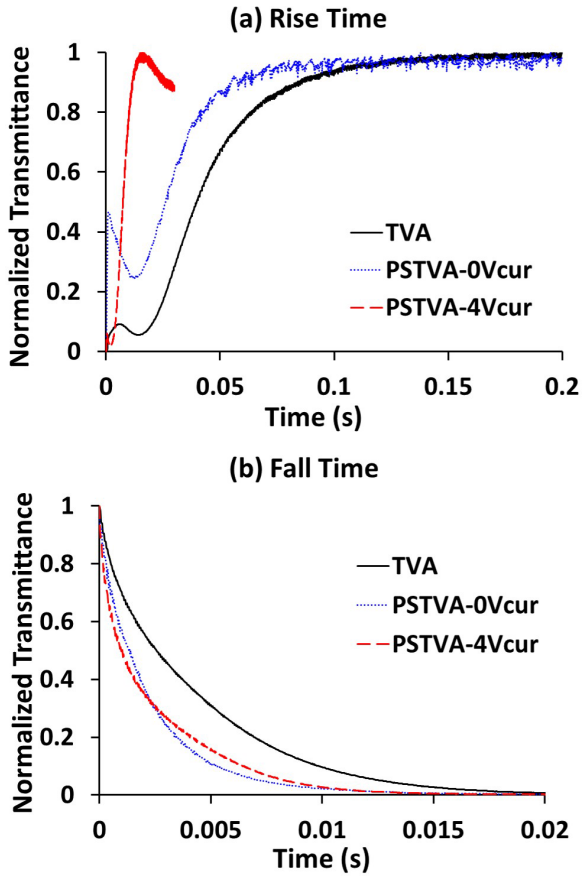

FIG. 5. Dynamic responses of the TVA and PS-TVA cells: (a) rise time and (b) fall time.

contrast ratio. The improved response time with suppressed optical bounce appears only when the polymerization voltage is higher than the threshold voltage. However, when the polymerization voltage is larger than the threshold voltage, the dark state light leakage at normal incidence increases because the polymerized twist structure increases phase retardation and induces rotation of light polarization. Therefore, to choose an optimized polymerization voltage, one should characterize the static voltage response before polymerization and choose the voltage that is larger than the threshold voltage but smaller than the applied voltage that gives 5% of transmittance.

The polymer microstructures of PS-TVA mode with different curing voltages are obtained using a scanning electron microscope (SEM, Hitachi S-2600N) and shown in Fig. 6.

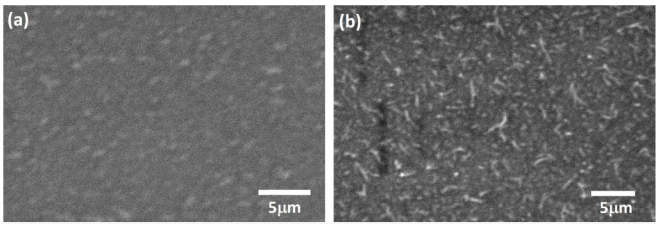

FIG. 6. Surface morphologies PS-TVA with different curing voltage (a) 0 V and (b) 4 V curing (threshold voltage before polymerization: 2.15 V).

The diameter of the polymer structure is 60–80 nm, and the length of polymer fiber ranges from hundreds of nanometers to 2–3 μm. The polymer structure is slightly larger when the curing voltage is smaller than threshold voltage [Fig. 6(a)]. From the static voltage response in Fig. 2(a), the two conditions exhibit different driving voltages. We speculate that it is resulting from the effective aligning field from the polymer structure and discuss further from the aspect of free energy density of the system.

The free energy density f of the whole system can be written as

$$f = f_{\text{elastic}} + f_p + f_{\text{electric}} \tag{1}$$

where f_{electric} is the elastic free energy density, f_p is the free energy density from the interaction between liquid crystal and polymer structure, and f_{electric} is electric free energy density. The free energy density contributed by the elastic distortion can be expressed with the Oseen-Frank energy equation with one elastic constant K approximation and variation at the z axis:

$$f_{\text{elastic}} = \frac{1}{2}K\left[\left(\frac{\partial n_x}{\partial z}\right)^2 + \left(\frac{\partial n_y}{\partial z}\right)^2 + \left(\frac{\partial n_z}{\partial z}\right)^2 - 2q_0\left(-n_x\frac{\partial n_y}{\partial z} + n_y\frac{\partial n_x}{\partial z}\right) + q_0^2\right] \tag{2}$$

where n_x,n_y, and n_z are the components in the Cartesian coordinate in the liquid-crystal director $\vec{n} = (n_x,n_y,n_z)$. q_0 is the chirality which is equal to $2\pi/p$, where p is the pitch of the chiral nematic liquid crystal.

For f_p, following an approach proposed in Ref. [21], we model the alignment contributed by the polymer structure by an effective aligning field $\vec{E}_{\text{eff}}$. The free energy density f_p is assumed to be equal to the energy f_{eff} of the interaction between the liquid crystal and this effective field, such that f_{eff} is of the form

$$f_{\text{eff}} = \tfrac{1}{2}\varepsilon_0\Delta\varepsilon(\vec{E}_{\text{eff}}\cdot\vec{n})^2 \tag{3}$$

where ε_0 is the dielectric permittivity of the vacuum, $\Delta\varepsilon$ is the dielectric anisotropy of the liquid crystal, and $\vec{n}$ is the liquid-crystal director. Note that the aligning force from the polymer structure is independent of the dielectric anisotropy ($\Delta\varepsilon$) of the liquid crystals. The $\Delta\varepsilon$-dependent Eq. (3) is to find the external field required to overcome the aligning force [21]. In this paper, the liquid-crystal molecules tend to align parallel to the polymer structure owing to the rigid core in reactive mesogens. f_{eff} is minimized when the angle between $\vec{E}_{\text{eff}}$ and $\vec{n}$ is zero with liquid crystal of negative dielectric anisotropy. The direction normal to the substrate is defined as the z axis. The electric free energy density f_{electric} can be written as

$$f_{\text{electric}} = -\tfrac{1}{2}\varepsilon_0\Delta\varepsilon(\vec{E}\cdot\vec{n})^2 \tag{4}$$

The direction of electric field $\vec{E}$ is fixed at the z axis which is perpendicular to the substrate. In PS-TVA mode we use negative liquid crystal. Therefore, the lowest free energy density contributed by the electric field appears when the director is perpendicular to the electric field. The director $\vec{n}$

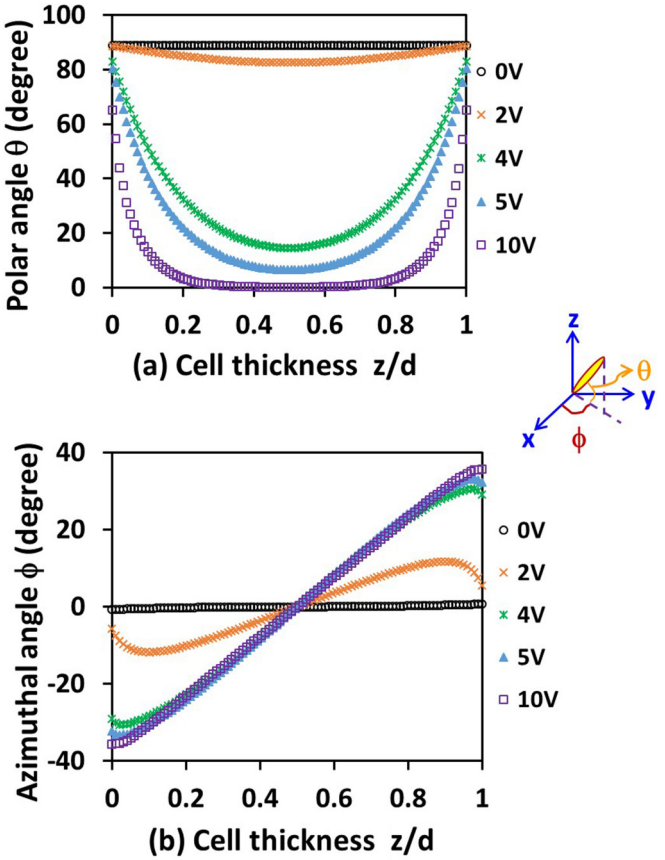

FIG. 7. (a) Tilt angle of TVA mode and (b) twist angle of TVA mode at different applied voltages.

can be expressed by

$$\vec{n} = \begin{pmatrix} \cos\theta(z,V)\cos\phi(z,V) \\ \cos\theta(z,V)\sin\phi(z,V) \\ \sin\theta(z,V) \end{pmatrix} \tag{5}$$

where $\theta(z,V)$ is the angle from the substrate and $\phi(z,V)$ is the azimuthal angle from the x axis on the x-y plane. Both angles are functions of applied voltage V and cell depth z. An illustration of angle definition is inserted in Fig. 7.

The liquid-crystal director as a function of cell depth z and applied voltage is simulated by Techwiz 2D LCD (SANAYI system, Co., Ltd.) as shown in Fig. 7, which is used for free energy calculation. The direction of effective aligning field contributed by the polymer structure depends on the polymerization voltage and cell depth. The aligning field $\vec{E}_{\text{eff}}$ with the amplitude E_{eff} follows the liquid-crystal director at the curing voltage V_{cur}:

$$\vec{E}_{\text{eff}} = E_{\text{eff}} \begin{pmatrix} \cos[\theta(z,V_{\text{cur}})]\cos[\phi(z,V_{\text{cur}})] \\ \cos[\theta(z,V_{\text{cur}})]\sin[\phi(z,V_{\text{cur}})] \\ \sin[\theta(z,V_{\text{cur}})] \end{pmatrix}. \tag{6}$$

The magnitude of aligning field of the polymer network E_{eff} can be described by [21]

$$E_{\text{eff}} = \left(\frac{\pi^3 K}{(8+\pi^2)\varepsilon_0|\Delta\varepsilon|}\right)^{\frac{1}{2}} \frac{\sqrt{c}}{R} \tag{7}$$

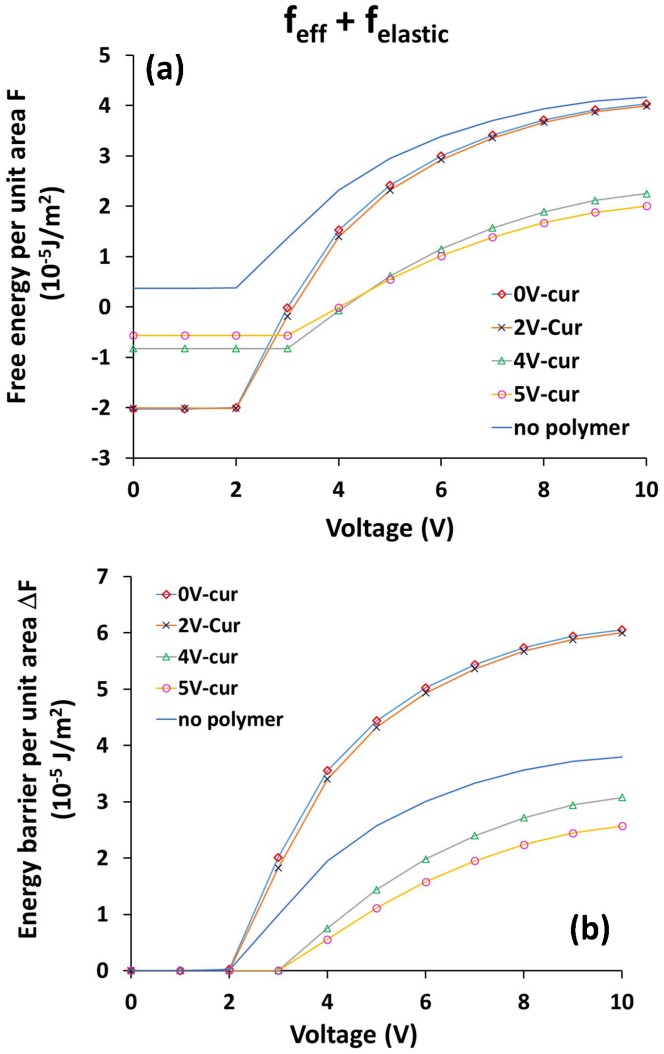

FIG. 8. (a) Free energy per unit area. (b) Energy barrier for achieving liquid-crystal director profile at voltage = V.

where K is the effective elastic constant, c is the polymer concentration, and R is the radius of the polymer fibers. The calculated magnitude of the effective aligning field from the polymer structure E_p is 0.57 V/μm. The free energy density is integrated along the z axis (which becomes free energy per unit area) and the energy barrier is calculated and presented in Figs. 8(a) and 8(b). For the free energy discussion and energy barrier calculation, we use the simulated director profile from Fig. 7. The simulated director profile is TVA mode without polymer structure under different applied voltages. We could use the director to calculate the elastic free energy and the contribution from the aligning field of the polymer structure using Eqs. (2) and (3). The free energy calculation does not include the contribution from the electric field. We calculate the sum of elastic free energy and contribution from polymer structure to have a qualitative idea of the driving voltage. In Fig. 8(a), free energy per unit area decreases in the presence of polymer with the curing voltage lower than the threshold voltage. Without polymer structure, at voltage = 0 V, the system exhibits small twist which is resulting from the chiral dopant. The free energy per unit area is not zero at voltage = 0 V in Fig. 8(a) which may come from the one elastic constant

approximation. Suppose the liquid crystals align parallel to the polymer structure completely, i.e., the angle between $\vec{E}_{\text{eff}}$ and $\vec{n}$ is zero. The free energy density from the interaction between polymer and liquid crystal is nonzero and hence lowers the free energy density at the ground state. Extra energy is required to induce the Freedericksz transition. Therefore, the threshold voltage increases, which is observed experimentally.

The energy barrier for switching the liquid-crystal director from the state voltage = 0 to voltage = V is the difference between free energy per unit area of voltage = 0 and of voltage = V. We calculate the energy barrier from Fig. 8(a) as shown in Fig. 8(b). With curing voltage smaller than threshold voltage, the energy barrier to achieve voltage = V is higher than that for the sample without polymer structure, and therefore we observed an increase of driving voltage experimentally. When the curing voltage is larger than the threshold voltage, the energy barrier is smaller than that for the sample without polymer structure. Experimentally we observed a decrease of driving voltage in PS-TVA with curing voltage 5 V. The free energy calculation gives a qualitative explanation for the observed driving voltage dependence on the polymer structure. It is simplified to single axis director variation and one elastic constant approximation to reduce the computation time.

In summary, we report a fast-switching liquid-crystal mode with polymer-sustained twisted vertical alignment. With optimized polymerization condition, the polymer-sustained alignment eliminates the pretilt angle degeneracy and suppresses the optical bounce, which are the original causes for slow dynamic response and flickering. The total response time has 83% improvement comparing with TVA mode without polymer-sustained alignment. Simultaneously, the PS-TVA cells also provide a very high optical contrast at a ratio of 1300:1 with achromatic bright state as that of a twist nematic cell. The driving voltage affected by the polymer structure depends on the applied voltage during polymerization. When the curing voltage is larger than threshold voltage, the energy barrier for achieving the same director profile decreases. The outcomes of this paper will enable the development of fast-switching and achromatic electro-optical and photonic devices.

The authors gratefully acknowledge the technical support provided by Dr. Min Gao and Dr. Lu Zou for scanning electron microscopy experiments at Ohio Research Center of Self-Assembled Material Characterization Facilities of Liquid Crystal Institute. This work was supported by the Ohio Third Frontier (OTR) Venture Startup Fund under Grant No. TECG 2015-0128.

[1] C. Rosenblatt, M. R. Fisch, K. A. Crandall, and R. Petschek, US Patent No. 5 477 358 (19 December 1995).
[2] K. A. Crandall, M. R. Fisch, R. G. Petschek, and C. Rosenblatt, Appl. Phys. Lett. **65**, 118 (1994).
[3] K. A. Crandall, M. R. Fisch, R. G. Petschek, and C. Rosenblatt, Appl. Phys. Lett. **64**, 1741 (1994).
[4] S.-T. Wu, C.-S. Wu, and K.-W. Lin, J. Appl. Phys. **82**, 4795 (1997).
[5] D.-K. Yang, L.-C. Chien, and J. W. Doane, Appl. Phys. Lett. **60**, 3102 (1992).
[6] J.-S. Hsu, B.-J. Liang, and S.-H. Chen, Appl. Phys. Lett. **85**, 5511 (2004).
[7] B. Taheri, D. Baker, E. Bardun, T. Kosa, L. Sukhomlinova, and P. Luchette, US Patent No. 2014/0226096 A1 (14 August 2014).
[8] Y.-H. Lee, K.-C. Huang, W. Lee, and C.-Y. Chen, J. Display Tech. **10**, 1106 (2014).
[9] L.-Y. Chen and S.-H. Chen, J. Soc. Inf. Disp. **7**, 289 (1999).
[10] M. Gu, I. I. Smalyukh, and O. D. Lavrentovich, Appl. Phys. Lett. **88**, 061110 (2006).
[11] S. H. Lee, S. M. Kim, and S.-T. Wu, J. Soc. Inf. Disp. **17**, 551 (2009).
[12] S. H. Kim and L.-C. Chien, Jpn. J. Appl. Phys. **43**, 7643 (2004).
[13] L. Weng, P.-C. Liao, C.-C. Lin, T.-L. Ting, W.-H. Hsu, J.-J. Su, and L.-C. Chien, AIP Advances **5**, 097218 (2015).
[14] S. H. Kim, L.-C. Chien, and L. Kopmitov, Appl. Phys. Lett. **86**, 161118 (2005).
[15] T. Kosa, V. H. Bodnar, B. Taheri, and P. Palffy-Muhoray, Mol. Cryst. Liq. Cryst. **369**, 129 (2001).
[16] J. Chen, P. J. Bos, D. L. Johnson, D. R. Bryant, J. Li, S. H. Jamal, and J. R. Kelly, J. Appl. Phys. **80**, 1985 (1996).
[17] A. Takeda, S. Kataoka, T. Sasaki, H. Chida, H. Tsuda, K. Ohmuro, T. Sasabayashi, Y. Koike, and K. Okamoto, SID Symposium Digest Technical Papers **29**, 1077 (1998).
[18] J. Chen, K.-H. Kim, J.-J. Jyu, J. H. Souk, J. R. Kelly, and P. J. Bos, SID Symposium Digest of Technical Papers **29**, 315 (1998).
[19] Y. Gao, Z. Luo, R. Zhu, Q. Hong, S.-T. Wu, M.-C. Li, S.-L. Lee, and W.-C. Tsai, J. Display Technol. **11**, 315 (2015).
[20] S.-H. Chen and L.-Y. Chen, Appl. Phys. Lett. **75**, 3491 (1999).
[21] D.-K. Yang and S.-T. Wu, *Fundamentals of Liquid Crystal Devices*, 2nd ed. (Wiley, New York, 2015).